JOURNAL OF CATALYSIS 138, 195–205 (1992)

Effect of the Preparation Method on the Thermal Stability of Silica-Supported Nickel Oxide as Studied by EXAFS and TPR Techniques

O. CLAUSE,*[,1] L. BONNEVIOT,†[,2] AND M. CHE†

*Institut Français du Pétrole, Division Cinétique et Catalyse, 1 avenue de Bois-Préau BP 311, 92506 Rueil-Malmaison, France; and †Laboratoire de Réactivité de Surface et Structure, URA 1106 CNRS, Université Pierre et Marie Curie, 4 place Jussieu, 75252 Paris Cedex 05, France

Received December 3, 1991; revised July 1, 1992

EXAFS analysis and Temperature-Programmed Reduction experiments (TPR) have been carried out on calcined Ni/SiO_2 materials prepared by incipient wetness impregnation at different pH values, ion exchange with ammonia and ethylenediamine solutions, and deposition–precipitation. The interaction of the Ni(II) ions with silica is shown to be dependent on the first steps of catalyst preparation, i.e., deposition, washing, and drying. Silicates with a layer structure are formed in samples prepared by deposition–precipitation and ion exchange from ammoniacal solutions. Silicate formation inhibits the NiO crystallization up to 500°C. The silicate decomposition is favored when the thermal treatment is performed under reduced pressure. The reducibility of the nickel oxide phase resulting from silicate decomposition is strongly hindered in comparison with that of unsupported nickel oxide. The silicate formation is avoided using a strong chelating ligand such as ethylenediamine during ion exchange. With ethylenediamine, isolated Ni(II) species stable to 500°C are obtained.

INTRODUCTION

Silica-supported nickel catalysts have found widespread application in hydrogenation and hydrogenolysis reactions, such as the methanation of coal synthesis gas (*1–3*), or in olefin dimerization (*4, 5*). It is well known that the preparation method has a significant effect on the properties of Ni/SiO_2 catalysts, such as reducibility and Ni particle size distribution. For example, Ni/SiO_2 catalysts prepared by incipient wetness impregnation or by deposition–precipitation have been shown to present quite different behavior upon reduction/oxidation treatments (*6–8*). In the former case, large NiO crystallites are formed upon calcination, leading to large nickel particles and broad size distributions after reduction. In the latter, finely dispersed and evenly distributed nickel particles are obtained. This has been suggested to result from the formation of nickel "hydrosilicate" layers during the deposition–precipitation, thus limiting the coalescence of large nickel particles upon reduction. Nickel catalysts with homogeneous particle sizes were also prepared by the sol–gel method involving the hydrolysis of a mixed solution of ethyl silicate and Ni(II) nitrate in ethylene glycol followed by suitable calcination and reduction treatments (*9, 10*).

The importance of the operations preceding reduction, i.e., impregnation, washing, drying, and calcination steps, is thus emphasized and more insight on their respective role is clearly needed. In previous papers, we focused our attention on the impregnation, washing, and drying steps for the preparation of Ni/SiO_2 materials by deposition–precipitation (*11*), impregnation from Ni(II) ammine solutions with and without washing (*12*), and ion exchange from Ni(II) ethylenediamine solutions (*13*). A detailed

[1] To whom correspondence should be addressed.

[2] Present address: Departement de Chimie, Université Laval, G1V 1E6, Québec, Canada.

0021-9517/92 $5.00

description of the adsorbed state of the Ni(II) ions was obtained using UV–visible, IR, and XAS spectroscopies. During deposition–precipitation, silicates with a layer structure are formed, independent of the Ni content. No $Ni(OH)_2$ epitaxially deposited onto the silicate layers is observed by EXAFS in the washed samples. Ion exchange from Ni(II) ammoniacal solutions also leads to silicates with a layer structure, either during the impregnation or the drying steps, depending on the pH of the solutions. The hexaamminenickel(II) complexes adsorb electrostatically onto the silica surface during impregnation. Then, the removal of the ammine ligands from the Ni(II) coordination sphere during drying at ambient temperature leads to Ni(II) silicate formation. Silicate formation is avoided using chelating ligands such as ethylenediamine instead of ammonia. Incipient wetness impregnations with ammoniacal Ni(II) solutions lead to a mixture of Ni(II) nitrate salt trapped in the pores of the support and layered Ni(II) silicates, depending on the pH of the solutions. The silica is suggested to act as a dispersing agent for acidic pH impregnation (pH < 4), whereas Ni(II) silicates are formed when the pH is near 8.3.

This paper examines the calcination step. In particular, we are concerned with the thermal stability of isolated Ni(II) species grafted onto silica by ion exchange from Ni(II) ethylenediamine solutions. Likewise, the reducibility of the NiO resulting from the thermal decomposition of Ni(II) silicates is studied. A detailed description of the Ni(II) state during the various steps of the preparations techniques listed above is presented in the Discussion.

TABLE 1

Preparation Procedures and Nickel Contents of Samples A–G

Sample	Preparation procedure	Nickel content (wt%)[a]	Ref.
A	Incipient wetness impregnation Solution at pH 5.7 and (NH_4NO_3) = 1 *M* Drying at 120°C	1.4	(*12*)
B	Incipient wetness impregnation Solution at pH 6.9 and (NH_4NO_3) = 1 *M* Drying at 120°C	1.4	(*12*)
C	Incipient wetness impregnation Solution at pH 8.3 and (NH_4NO_3) = 1 *M* Drying at 120°C	1.4	(*12*)
D	Incipient wetness impregnation Solution at pH 10.2 and (NH_4NO_3) = 1 *M* Drying at 120°C	1.4	(*12*)
E	Ion exchange with an Ni(II) ammoniacal solution at pH 9.8 and (NH_4NO_3) = 1 *M* Drying at 120°C	1.1	(*12*)
F	Deposition–precipitation (urea decomposition) Drying at 120°C	7.5	(*11*)
G	Ion exchange with an Ni(II) ethylenediamine solution at pH 9.3 Drying at 120°C	1.1	(*13*)

[a] As determined by atomic absorption after acid extraction.

EXPERIMENTAL

Ni/SiO_2 samples were prepared by incipient wetness impregnation, ion exchange, and deposition–precipitation techniques; see Table 1. Details on the preparation parameters can be found in the references listed in Table 1.

The heating was performed in a tubular furnace in air or *in vacuo* (reduced pressure: 20 Pa). The calcination temperature was increased with a heating rate of 5°C/mn then kept at the desired value for 16 hr. The nickel contents of the samples calcined at 650°C were measured by atomic absorption after acid extraction and are reported in Table 1.

The TPR measurements were performed in an apparatus described previously (*11*).

The heating rates were 7.5°C/min and the reducing mixture was 5% H_2 in argon (Air Liquide).

The EXAFS measurements were performed at the LURE radiation synchrotron facility on X-ray beamline D44 emitted by the DCI storage ring (positron energy, 1.85 GeV; ring current, 300 mA). The spectra were recorded in transmission mode at ambient temperature using two air-filled ionization chambers. The monochromator was a channel-cut single crystal of silicon, the (331) reflexion being used. The resolution $\delta E/E$ at the Ni K-edge was 2×10^{-4}. The energies were scanned with 2-eV steps from 100 eV below up to 700 eV above the Ni K-absorption-edge. The samples were in powder form screened to 60–130 μm. The sample thicknesses were chosen such that the edge jump heights (μx variation through the edge, μ being the linear absorption coefficient) ranged from 1.0 to 1.5. The Ni(II) absorption was obtained by fitting the pre-edge absorption curve with a Victoreen's function and extrapolating the absorption beyond the edge, then subtracting the theoretical from the experimental absorption (*14*). A polynomial spline procedure was then used for background removal and normalization. The origin of energies was identified to the maximum of the absorption derivative. The data in k-space were Fourier transformed over a 3 to 12 $Å^{-1}$ Hanning window after weighting by a k^3 factor. The fittings were performed simultaneously in the k- and R-spaces, using reference compounds for the determination of the backscattering phase and amplitude functions. Pure NiO, a well-crystallized $Ni(OH)_2$ sample, and an Ni-doped magnesium hydroxide sample were chosen as references for the Ni–O, the Ni–Ni, and the Ni–Si systems, respectively; see Table 2 (*11–13, 15, 16*).

TABLE 2

Structural Parameters of References and Samples E and G as Determined by EXAFS Spectroscopy at the Ni K-edge

Sample	Shell atom	Distance (Å)	Number	σ (Å)	Q
NiO	O	2.09	6	0.090	
$Ni(OH)_2$	Ni	3.13	6	0.090	
Ni : $Mg(OH)_2$	Mg	3.13	6	0.090	
Sample E, 120°C	O	2.04	6.0	0.090	0.001
	Ni	3.10	6.0	0.097	
	Si	3.31	1.9	0.065	0.0016
Sample E, 500°C	O	2.04	5.7	0.098	0.0003
in air	Ni	3.09	4.8	0.104	
	Si	3.23	4.8	0.075	0.0070
Sample E, 700°C	O	2.04	5.7	0.103	0.0003
in air	Ni	3.08	3.0	0.104	
	Si	3.25	4.2	0.075	0.0042
Sample E, 700°C	O	2.03	5.0	0.098	0.001
in vacuum	Ni	3.05	0.9	0.100	
	Si	3.33	4.1	0.083	0.0061
Sample G, 500°C	O	2.02	5.0	0.100	0.001
in air	Ni	3.03	0.55	0.098	
	Si	3.27	2.8	0.090	0.0088

Note. The best fits are obtained by minimizing the agreement factor Q. The mean free path parameter is taken equal for all samples. The precision on the distances is ±0.05 Å. The precision on the backscatterer numbers is ±0.5. The precision on the Debye–Waller factors is ±0.005.

RESULTS

Samples Prepared by Incipient Wetness Impregnation

The TPR profiles of samples A, B, C, and D calcined at 500°C are presented in Fig. 1. The reduction profile of a well-crystallized NiO sample obtained by calcination of nickel nitrate at 500°C is also shown. It appears that the pH of the impregnating solution plays a major role in the reducibility of the calcined samples. The reduction profiles of samples A and D resemble that of NiO, suggesting that Ni(II) is mainly present as NiO crystallites in these samples. Sample B is quantitatively reduced only at temperatures higher than 800°C, even though the maximum of the profile is close to that of unsupported NiO. Sample C exhibits a different reduction behavior, with two hydrogen uptake maxima around 620 and 820°C. The determination of Ni species from TPR by itself is a difficult problem (see Discussion). A previous study has shown that the Ni(II) ions form layered silicates in dried sample C (*12*). The complex TPR profile of sample C calcined at 500°C may be due to the reduction of the thermal decomposition products of layered Ni(II) silicates. Reduction profiles exhibiting two hydrogen con-

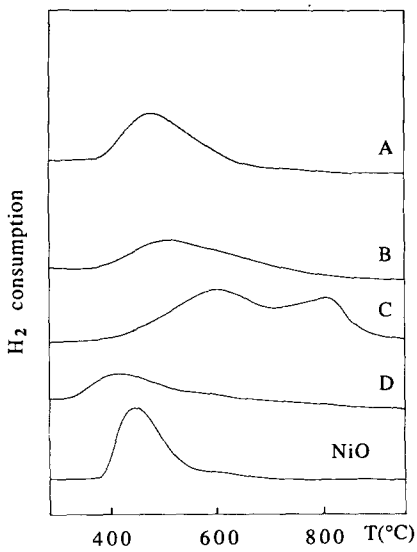

FIG. 1. TPR profiles unsupported NiO and of samples A, B, C, D prepared by incipient wetness impregnation (see Table 1) then calcined at 500°C.

sumption maxima have already been observed in nickel-silicate-containing samples (*17, 18*). pH values higher than 11 were not tested since strongly basic pH values are known to be aggressive for silica (*19*).

The Fourier transforms of the EXAFS spectra of NiO and sample A calcined at 500°C are shown in Fig. 2. The spectra are identical, thus the presence of NiO crystallites in sample A calcined at 500°C is confirmed. This sample being X-ray amorphous, the EXAFS technique appears to be more sensitive than XRD in detecting small nickel oxide crystallites.

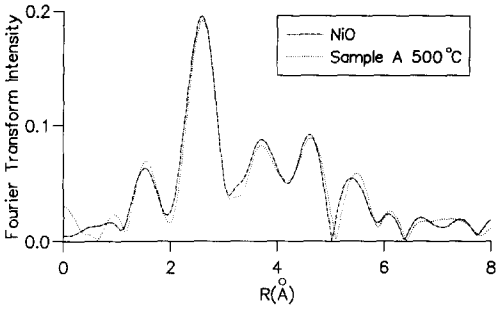

FIG. 2. Fourier transformed EXAFS spectra (k^3 weighted; without phase correction) of sample A calcined at 500°C and of unsupported NiO.

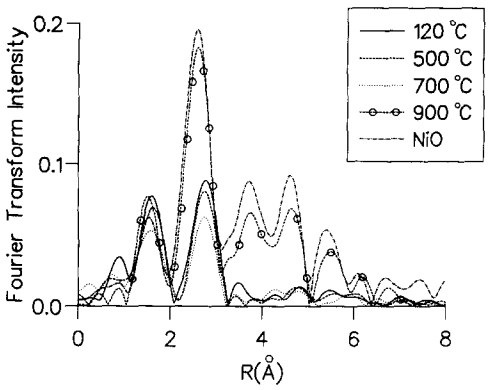

FIG. 3. Fourier transformed EXAFS spectra (k^3 weighted; without phase correction) of sample E prepared by ion exchange from ammoniacal solution, dried at 120°C, calcined at 500, 700, and 900°C, and of unsupported NiO.

Sample Prepared by Ion Exchange from an Ammoniacal Solution

The Fourier transforms of the EXAFS spectra for sample E dried at 120°C and calcined at 500, 700, 900°C along with NiO are shown in Fig. 3. The spectrum of the dried sample has been already discussed in Ref. (*12*) in conjunction with IR experiments. Layered nickel silicates are present. The Ni(II) ions are surrounded by six oxygen backscatterers at 2.04 Å, six Ni backscatterers at 3.1 Å, and 1.9 Si at 3.3 Å; see Table 2. Upon calcining to 700°C, a slight evolution of the spectra is observed. The intensity of the nearest neighbor peak decreases, whereas its width increases, suggesting an increase of the static disorder around the Ni(II) ions in calcined samples. The increase of the disorder is accounted for by a slight increase of the Debye–Waller factor; see Table 2. The intensity of the next-nearest peak slightly decreases, but the spectra do not present the characteristic features of the NiO spectrum (Fig. 2). By contrast, the spectrum of sample E calcined at 900°C is visibly similar to that of nickel oxide. The

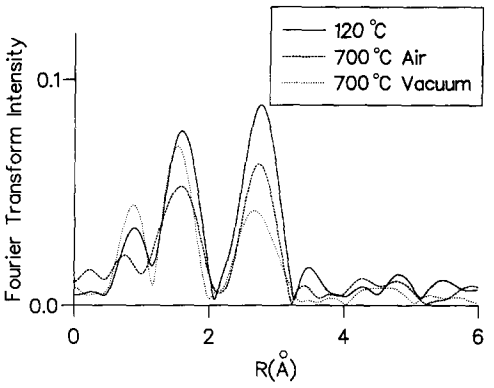

FIG. 4. Fourier transformed EXAFS spectra (k^3 weighted; without phase correction) of sample E heated at 120 and 700°C in air and at 700°C under vacuum.

EXAFS data clearly suggest that no NiO is formed upon calcination of sample E up to 700°C, whereas higher temperatures lead to a rearrangement of the Ni(II) ions with NiO formation. The presence of a small amount of nickel silicates in sample E calcined at 900°C, in addition to NiO may not be excluded. Indeed, the first coordination shell around the Ni(II) ions in NiO and silicates with layer structure is nearly the same (six oxygen backscatterers at distances ranging from 2.04 to 2.09 Å). The second coordination shell around the Ni(II) ions in layered silicates (six Ni and two or four Si backscatterers at distances ranging from 3.05 to 3.3 Å) may be difficult to observe when NiO particles are present (12 Ni backscatterers at 2.94 Å).

The Fourier-transformed EXAFS spectra of sample E heated in air at 120 and 700°C and under vacuum at 700°C are presented in Fig. 4. Heating *in vacuo* rather than in air visibly leads to a more pronounced decrease of the height of the second shell peak. No NiO phase is, however, detected.

The determination of the composition of the second coordination shell around Ni(II) ions after calcination gives information on the thermal decomposition of the silicates. Two synthetic and well-crystallized nickel silicates with layered structures, a nepouite and a nickel talc, were used in order to select correct values for the Debye–Waller factors (*11*). The Ni backscatterer contribution dominates at high photoelectron energies whereas that of Si dominates at low photoelectron energies (*12*). The Fourier backtransforms of the next-nearest neighbor peaks of sample E dried at 120°C and after heat treatment *in vacuo* at 700°C are shown in Fig. 5. It is apparent that, after heating in vacuum, the EXAFS signal is more attenuated at high energy values. This attenuation may be due to a diminution of the Ni neighbor number and/or an increase of the corresponding Debye–Waller damping factor. In a way opposite to that observed for high energy values, the amplitude of the EXAFS signal is enhanced at low energy values. The backscattering amplitude becomes close to that corresponding to Si backscatterers only (*12*). A fit is proposed in Table 2. The precision on the Si and Ni neighbor numbers (±0.5; see Table 2) is poor since the system presents a large disorder ($\sigma_{Ni} > 0.1$) and since oxygen backscatterers may also account for the enhancement of the signal at low energy values. However, the drastic diminution of the Ni backscatterer number indicates both the decomposition of the silicates layers and a "redispersion" of the Ni(II) ions. This trend is less apparent in the samples heated in air up to 700°C.

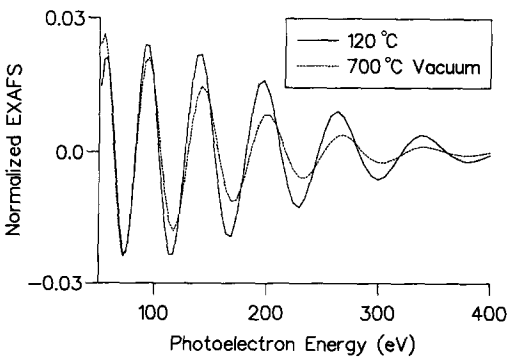

FIG. 5. Fourier backtransform of the next nearest neighbor peak in Fig. 4 of sample E dried at 120°C and sample E heated under vacuum at 700°C.

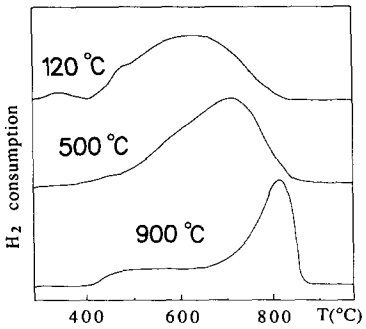

FIG. 6. TPR profiles of sample E dried at 120°C and calcined at 500 and 900°C.

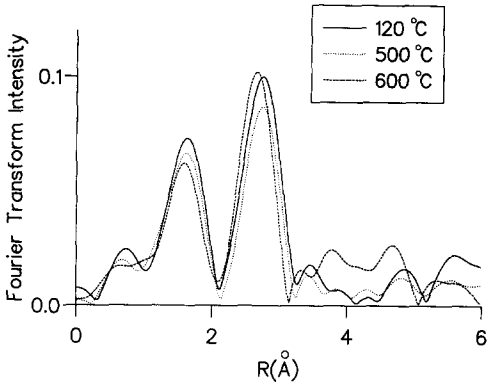

FIG. 7. Fourier transformed EXAFS spectra (k^3 weighted; without phase correction) of sample F prepared by deposition–precipitation, dried at 120°C, and calcined at 500 and 600°C.

The TPR profiles of sample E dried at 120°C and calcined at 500 and 900°C are shown in Fig. 6. Sample E exhibits a very broad reduction peak around 650°C. This profile appears similar to that observed during the reduction of synthetic nickel antigorite (*20, 17, 18*). Hence, the reduction behavior is consistent with the EXAFS analysis showing that the major part of Ni(II) ions forms nickel silicates. Upon calcination, sample E becomes even less reducible (see Fig. 6), in agreement with previous observations (*21*). When the calcination temperature reaches 900°C, the reduction extends to very high temperatures (830°C), even though EXAFS shows that the main part of Ni(II) is present as nickel oxide in the sample. The reducibility of this NiO phase is unusually low and strongly hindered in comparison to that of unsupported nickel oxide.

Sample Prepared by Deposition–Precipitation

The Fourier-transformed EXAFS spectra of sample F dried at 120°C then calcined at 500 and 600°C are shown in Fig. 7. After drying, the spectra of samples E (Fig. 3) and F are very similar. A detailed investigation of the Ni(II) environment in Ni/SiO_2 materials prepared by deposition–precipitation then washed with distilled water has revealed that the major part of the Ni(II) ions form nepouite-type silicates and that $Ni(OH)_2$ is not present in detectable amount (*11*). The thermal evolution of these silicates is similar to that of silicates present in sample E: no NiO phase formation is detected up to 500°C. When the calcination temperature reaches 600°C, however, the characteristic features of NiO are observed in the 3–5 Å range (see EXAFS spectrum of NiO in Fig. 3 for comparison).

The TPR profile obtained for dried sample F (see Fig. 8) is similar to those obtained in previous studies on Ni/SiO_2 catalysts pre-

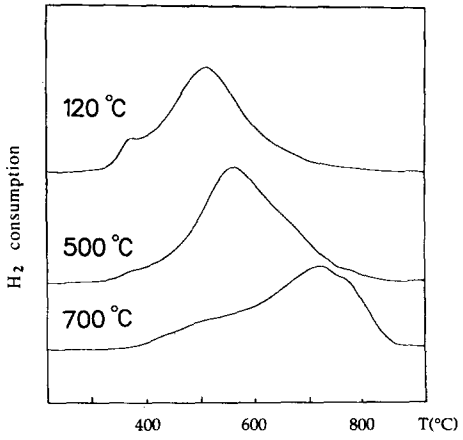

FIG. 8. TPR profiles of sample F dried at 120°C and calcined at 500 and 700°C.

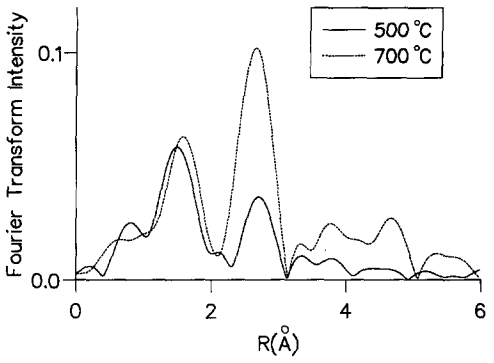

FIG. 9. Fourier transformed EXAFS spectra (k^3 weighted; without phase correction) of sample G prepared by ion exchange from an ethylenediamine solution and calcined at 500 and 700°C.

pared by deposition–precipitation (*8, 18, 22–24*). The higher the calcination temperature, the more difficult it is to reduce the sample. As in the case of sample E, the Ni(II) reducibility is not enhanced when a nickel oxide phase is formed.

Sample Prepared by Ion Exchange from an Ethylenediamine Solution

A previous EXAFS study (*13*) has shown that the nickel silicate formation is inhibited by the use of a ligand such as ethylenediamine. Isolated, grafted Ni(II) species are formed upon calcination at 300°C. These species are characterized by two silicon backscatterers located at 3.30 Å. The grafting site is a pair of vicinal silanol groups. The Fourier-transformed EXAFS spectra of sample G calcined at 500 and 700°C are presented in Fig. 9. An NiO phase is observed only when the calcination temperature reaches 700°C. The composition of the second coordination shell around Ni(II) ions is reported in Table 2. Silicates are not detected at either the calcination temperature. On the contrary, the Ni(II) ions are grafted and well dispersed on the silica surface since the Ni(II) backscatterer number is lower than 1. This good dispersion of nickel ions onto the silica surface is preserved for calcination temperatures as high as 500°C.

The TPR profiles of sample G calcined at 500 and 700°C are presented in Fig. 10. A thermogravimetric analysis of sample G under flowing helium showed a steady weight loss up to 500°C assigned to organic fragments arising from ethylenediamine decomposition. Thus, calcination temperatures higher or equal to 500°C are required in order to quantitatively remove organic molecules from the surface of sample G. The measured H/Ni ratio is close to 2 for both profiles presented in Fig. 10. This shows that nickel is mainly present as Ni(II). Surprisingly, well-dispersed grafted Ni(II) ions appear to be as difficult to reduce as Ni(II) silicates; compare Figs. 8 and 10.

DISCUSSION

Stability of Supported Silicates

When the samples are prepared by ion exchange from Ni(II) ammoniacal solutions (sample E) or the deposition–precipitation technique (sample F), silicates with a layer structure are formed at the solid–liquid interface during the first steps of catalyst preparation, i.e., the impregnation or the drying

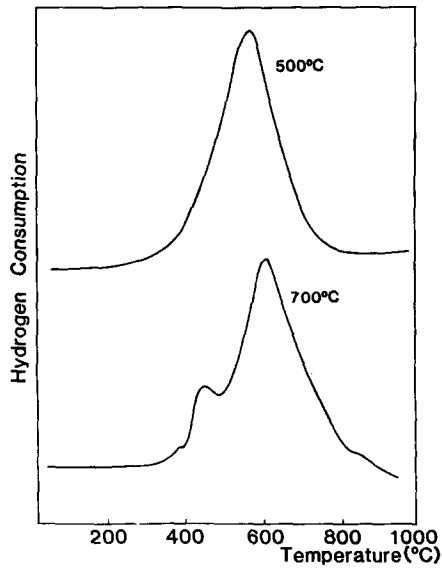

FIG. 10. TPR profiles of sample G calcined at 500 and 700°C.

steps (*11, 12*). The formation of layered structures is confirmed by other characterization techniques. In Ref. (*11*), an electron microscopy study showed the presence of thin platelets in Ni/SiO_2 samples prepared by deposition–precipitation and dried at 100°C. In Ref. (*12*), δ_{OH} bands characteristic for layered talc (716 cm^{-1}) or nepouite (670 cm^{-1}) structures were observed in Ni/SiO_2 samples prepared by ion exchange from ammoniacal solutions, before or after drying, depending on the pH of the exchange solutions. Other Ni silicates, such as Ni olivine which has the spinel structure, do not have such characteristic OH groups (*25*).

This paper characterizes the effect of calcination on silicate containing samples E and F. Silicates with a layer structure usually have a high thermal stability (*20*). The Ni(II) environment in samples calcined up to 500°C, as revealed by the EXAFS technique, appears similar to that observed after drying; see Figs. 3 and 7. The NiO phase is not present in detectable amount in these samples and silicates appear to be the main Ni(II) species present. The thermal decomposition of the supported silicates in samples E and F starts for calcination temperatures higher than 500°C and leads to the formation of nickel oxide. The decomposition temperature of supported silicates is similar to that of unsupported synthetized silicates (*20*). Regardless of the nickel content (samples E or F), calcination temperatures lower than 500°C do not substantially modify the local composition around the Ni(II) ions, as measured by EXAFS (Fig. 3). Interestingly, in sample E, the silicate thermal decomposition leads to a redispersion of the Ni(II) ions prior to NiO formation. This redispersion is accounted for by a nickel next-nearest backscatterer number around 1, instead of 6 in silicate structure, and is favored by heating *in vacuo* instead of air. Heating *in vacuo* may facilitate the water removal resulting from the dehydroxylation of the silicates (*20*). It is likely that well-dispersed Ni(II) species are only obtained for low Ni contents, since a substantial support surface area is required. The redispersion of Ni(II) is followed by the formation of small crystallites of NiO, as revealed by EXAFS. This formation is not detected by X-ray diffraction: the EXAFS technique is more effective than XRD for detecting small NiO particles. For higher nickel contents, as in sample F (7.5 Ni wt% instead of 1.1 Ni wt% in sample E), the decomposition of silicates leads directly to nickel oxide formation and no Ni(II) redispersion is observed.

Reducibility of the NiO Phase Formed upon Silicate Thermal Decomposition

The reduction of the NiO particles resulting from the decomposition of the supported silicates is unusually difficult; see Figs. 6 and 8. The question arises as to whether the hindered reducibility and more generally the thermal stability of the silica supported NiO particles are a surface (silica "skin" outside the NiO particles) or a "bulk" phenomenon, due to silicate ions present inside the particles. The first hypothesis is supported by similar studies on the Fe_3O_4/SiO_2 (*26, 27*), Fe_3O_4/Al_2O_3 (*28*), and NiO/Al_2O_3 (*29*) systems. The latter has been suggested for Ag-, Li-, (*30*) or Al-doped nickel oxide (*31*). We discuss these two hypotheses successively in view of the TPR and EXAFS results presented.

The presence of a silica "skin" partially covering the NiO particles may hinder the reduction of the nickel oxide phase (*32*). Furthermore, silicate ions in the surface region of NiO particles may significantly handicap the growing and crystallization of the nickel oxide phase. The following question arises: If present, where does the silica "skin" originate from? For silica-supported iron oxide, silica migration has been observed upon treatment in H_2O/H_2 gas mixtures (*33*), leading to strong oxide–oxide interactions between silica and magnetite (*26, 27*). The dehydroxylation upon thermal decomposition of layered silicates produces

water (*20*). Thus, silica migration during calcination leading to partially covered NiO particles may also be involved.

Another explanation for a silica "skin" formation can be suggested from our data. The thermal decomposition of layered nickel silicates leads to the formation of nickel oxide and silica. The silica phase resulting from silicate decomposition may remain in close proximity to the formed NiO particles, possibly partially covering them. Thus, the presence of silicate ions in the surface region of the NiO particles, as a consequence of silicate decomposition, is probable.

On the other hand, the presence of silicate ions trapped in the NiO particles can also provide an explanation for the unusually low reducibility of the nickel oxide phase, through a possible increase of the activation energy of reduction (*30, 31*). It is likely that the thermal decomposition of layered nickel silicates do not lead to pure nickel oxide. Si^{4+} impurities may be included in the NiO lattice. As the samples are X-ray amorphous whatever the calcination temperature, this assumption can unfortunately not be confirmed in view of a shift of the NiO lattice parameters. The presence of small amounts of silicon ions inside the NiO particles cannot be rejected from the EXAFS data. Thus, it is not possible to definitely conclude from the data, whether or not the difficult reducibility of the nickel oxide phase arises from the presence of silicon ions located inside the NiO particles, or on them. Nevertheless, since silicate decomposition is involved for the NiO formation, the presence of silica on the NiO particles provides a reasonable explanation for their thermal stability.

In short, for Ni/SiO_2 samples prepared by deposition–precipitation or ion exchange from ammoniacal Ni(II) solutions, layered silicates are formed during the impregnation or the drying step. The Ni(II) ions are not atomically dispersed on the silica surface. Further calcinations at temperatures below 500°C do not alter significantly the samples. Silicate decomposition takes place progressively for higher calcination temperatures. When the Ni content is low, a "redispersion" of the Ni(II) ions, is observed prior to NiO formation. This Ni(II) redispersion is favored by heating in vacuum instead of air. When the calcination temperature reaches 900°C, NiO particles are formed regardless of the nickel content. This NiO phase has an unusually large thermal stability, which is likely to be related to the decomposition of Ni(II) layered silicates, leading to the presence of silicon ions in the surface region of the NiO particles.

Role of pH on the Phases Present in Samples Prepared by Incipient Wetness Impregnation

The role of pH of the impregnating solution on Ni/SiO_2 materials prepared by incipient wetness impregnation confirms the EXAFS results obtained in a previous study (*12*). It was shown that a part of the Ni(II) ions reacts with silica to form nickel silicates, the other part recrystallizing in the pores of silica as nickel(II) nitrate. The fraction of Ni(II) ions reacting with silica is related to the pH of the impregnating solution, i.e., the type of Ni(II) ammine complex predominant in solution. For acidic impregnation ($pH < 5$), nickel is mainly present as nickel nitrate crystallized in the pores of the dried samples. By contrast, when the pH ranges from 8 to 8.5, silicates are the main Ni(II) species. For impregnation pH values ranging from 6 to 8.5, both nickel nitrate crystallites and nickel silicates are formed.

The TPR profiles presented in Fig. 1 can be interpreted assuming that nickel nitrate decomposes to nickel oxide upon calcination in air, while nickel silicates remain unmodified, as already observed for silicates calcined at 500°C in samples E and F. When the impregnation pH is acidic (sample A) or higher than 10 (sample D), the support acts as a simple dispersing agent. The NiO phase forms at low calcination temperature and is

weakly bonded to silica. Hence its reduction profile resembles that of unsupported nickel oxide. For impregnation pH near 8.3, calcining leads to a mixture of layered nickel silicates and nickel oxide supported on silica. It was suggested that nickel nitrate, basic nitrate or nickel oxide can react with silica during calcination to form silicates (*34, 35*). Silicate formation during calcination can not be excluded by our results, but it is probable that the main part of silicates is already formed during drying (*12*).

In short, Ni(II) is mainly present in NiO crystallites and Ni layered silicates in calcined Ni/SiO_2 materials prepared by incipient wetness impregnation. The fraction of NiO with respect to silicates is related to the composition of the impregnating solutions, i.e., pH and NH_3 concentration.

Influence of the Ligand in the Production of Isolated Grafted Ni(II) Ions

The use of ethylenediamine instead of ammonia as ligand for the ion-exchange process offers an interesting alternative, since silicate formation is avoided (*13*). Isolated, grafted Ni(II) species are obtained upon calcination and these species are stable up to 500°C. The removal of ethylenediamine from the silica surface and from the Ni(II) coordination sphere needs calcination temperatures higher than 500°C. No evidence for partial reduction of Ni(II) into Ni(I) or metallic nickel during the amine desorption is found. This can be explained by the oxidizing atmosphere used for heating. The EXAFS analysis indicates that layered nickel silicates are not formed during calcination. Even though silicates are not formed, the calcined samples are not readily reduced. Si–O–Ni bonds need to be broken for the Ni(II) ions to be reduced. This may explain why Ni silicates, as well as Ni(II) ions grafted on silica, are difficult to reduce. Likewise, the NiO formation upon calcination needs to cleave Si–O–Ni bonds. Hence it occurs at high temperatures for samples E and F as well as sample G.

Complementarity of TPR and EXAFS Experiments to Characterize Ni/SiO_2 Samples

The TPR and EXAFS techniques are well suited and complementary for the characterization of calcined Ni/SiO_2 materials. The EXAFS technique is more effective than X-ray diffraction for revealing the presence of layered nickel silicates as well as small nickel oxide particles. The thermal decomposition of silicates is monitored through a decrease of the Ni next-nearest backscatterer number. The grafting of isolated Ni(II) ions is characterized by the presence of silicon next nearest backscatterers. Thus, EXAFS provides useful information both on the ion–ion interactions (Ni–O–Ni bonds) and on the ion–support interactions (Ni–O–Si bonds) in calcined samples. However, EXAFS fails to evaluate the interactions between the nickel oxide phase and the support. The Fourier-transformed EXAFS spectra of sample A calcined at 500°C and sample E calcined at 900°C are similar; see Figs. 2 and 6. Nevertheless, the TPR profiles of these samples are quite different, indicating different interactions between the oxide phase and the support. This underlines the usefulness of the TPR technique. It should be mentioned, however, that TPR by itself is not sufficient to fully determine the Ni(II) species. Highly dispersed grafted Ni(II) species as well as partially decomposed silicates may account for TPR profiles between 500 and 700°C; see Figs. 8 and 10. Likewise, the maximum of the hydrogen consumption peaks at 500°C for NiO in sample A calcined at 500°C and at 830°C for NiO in sample E calcined at 900°C. Thus, TPR by itself cannot be used as a fingerprint of the presence of a given phase, nickel silicate or nickel oxide, for example, in Ni/SiO_2 samples.

CONCLUSION

The type of Ni(II) species present in calcined $Ni(II)/SiO_2$ materials appear to be mainly controlled by the ion–support interactions generated during the impregnation

and drying steps. When layered silicates are formed, i.e., during deposition–precipitation or ion exchange from ammoniacal solutions, the Ni(II) species observed in the calcined samples are the products of silicate decomposition. NiO is not formed for calcination temperatures below 500°C. Silicate formation is avoided using ethylenediamine instead of ammonia as ligand during ion exchange. With ethylenediamine, silicates are not formed at any calcination temperature and NiO is not formed for calcination temperatures lower than 600°C. By contrast, for incipient wetness impregnations with acidic nickel nitrate solutions, a nickel oxide phase is formed for calcinations below 500°C, indicating a weak interaction of the Ni(II) ions with silica.

ACKNOWLEDGMENTS

We express our thanks to M. Varin for assistance in graphic design, to Mme Russmann for assistance in TPR experiments, and to the LURE staff for help during EXAFS runs. Stimulating discussions with Dr. C. Cameron are gratefully acknowledged.

REFERENCES

1. Bell, A. T., "Catalyst Design: Progress and Perspectives," pp. 125, 134. Wiley, New York, 1987.
2. Randava, S. S., Camara, E. H., and Rehmat, H., *Ind. Eng. Chem., Prod. Res. Dev.* **8**(4), 347 (1969).
3. Mills, G. A., and Steffgen, F. W., *Catal. Rev.* **8,** 191 (1974).
4. Elev, I. V., Kazanski, V. B., and Shelimov, B. N., *J. Catal.* **89,** 470 (1984).
5. Bonneviot, L., Olivier, D., and Che, M., *J. Mol. Catal.* **21,** 415 (1983).
6. Richardson, J. T., Dubus, R. J., Crump, J. G., Desai, P., Sterwalder, U., and Cale, T. S., *in* "Preparation of Catalsyts II" (B. Delmon *et al.*, Eds.), p. 131. Elsevier, Amsterdam, 1979.
7. Blackmond, D. A., and Ko, E. I., *Appl. Catal.* **13,** 49 (1984).
8. Montes, M., Soupart, J. B., De Saedeleer, M., Hodnett, B. K., and Delmon, B., *J. Chem. Soc. Faraday Trans. 1* **80,** 3209 (1984).
9. Ueno, A., Suzuki, H., and Kotera, Y., *J. Chem. Soc. Faraday Trans. 1* **79,** 127 (1983).
10. Tohji, K., Udagawa, Y., Tanabe, S., and Ueno, A., *J. Am. Chem. Soc.* **106,** 612 (1984).
11. Clause, O., Bonneviot, L., Che, M., and Dexpert, H., *J. Catal.* **130,** 21 (1991).
12. Clause, O., Kermarec, M., Bonneviot, L., Villain, F., and Che, M., *J. Am. Chem. Soc.*, **114,** 4709 (1992).
13. Bonneviot, L., Clause, O., Che, M., Manceau, A., and Dexpert, H., *Catal. Today* **6,** 39 (1989).
14. Teo, B. K., "EXAFS: Basic Principles and Data Analysis," p. 116. Springer-Verlag, Berlin, 1986.
15. "Gmelins Handbuch der Anorganischen Chemie," Vol. B2, p. 392. Verlag-Chemie, Weinheim, 1966.
16. McEwen, R. S., *J. Phys. Chem.* **75,** 1782 (1971).
17. Lemaitre, J., and Gerard, P., *Bull. Mineral.* **104,** 665 (1981).
18. Wendt, G., and May, M., *Z. Chem.* **26,** 177 (1986).
19. Iler, R. K., "The Chemistry of Silica," p. 557. Wiley, New York, 1979.
20. Martin, G. A., Renouprez, A., Dalmai-Imelik, G., and Imelik, *J. Chim. Phys.* **67,** 1149 (1970).
21. Bhatia, S., Beltramini, J., and Do, D. D., *Catal. Today* **7,** 372 (1990).
22. Shyu, Z. L., Thesis, University of Pittsburgh, 1983.
23. Coenen, J. W. E., *Appl. Catal.* **54,** 65 (1989).
24. Gil, A., Diaz, A., and Montes, M., *J. Chem. Soc. Faraday Trans.* **87,** 791 (1991).
25. Wells, A. F., "Structural Inorganic Chemistry," p. 1015. Clarendon, Oxford, 1984.
26. Lund, C. R. F., and Dumesic, J. A., *J. Phys. Chem.* **85,** 3175 (1981).
27. Lund, C. R. F., and Dumesic, J. A., *J. Phys. Chem.* **86,** 130 (1982).
28. Jung, H., and Thomson, W., *J. Catal.* **128,** 218 (1991).
29. Clause, O., Rebours, B., Merlen, E., Trifiró, F., and Vaccari, A., *J. Catal.* **133,** 231 (1992).
30. Parravano, G., *J. Am. Chem. Soc.* **74,** 1194 (1952).
31. Puxley, P. C., Kitchener, I. J., Komodromos, C., and Parkyns, N. D., *in* "Preparation of Catalysts III" (G. Poncelet *et al.*, Eds.), p. 237. Elsevier, Amsterdam, 1983.
32. Bond, G. C., "Catalysis by Metals," p. 40. Academic Press, London, 1962.
33. Lund, C. R. F., and Dumesic, J. A., *J. Catal.* **72,** 21 (1981).
34. Mile, B., Stirling, D., Zammitt, M. A., Lovell, A., and Webb, M., *J. Catal.* **114,** 217 (1988).
35. Mile, B., Stirling, D., Zammitt, M. A., Lovell, A., and Webb, M., *J. Mol. Catal.* **62,** 179 (1990).